Publishing House
AKAPIT

COMPUTER METHODS IN MATERIALS SCIENCE
Informatyka w Technologii Materiałów

Vol. 17, 2017, No. 1

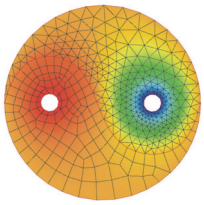

ANALYSIS OF BAINITE ONSET DURING COOLING FOLLOWING PRIOR DEFORMATION AT DIFFERENT TEMPERATURES

AARNE POHJONEN*, ANTTI KAIJALAINEN, MAHESH SOMANI, JARI LARKIOLA

University of Oulu, Pentti Kaiteran katu 1, 90014 Oulu, Finland
**Corresponding author: Aarne.Pohjonen@oulu.fi*

Abstract

Final rolling temperature affects the austenite grain structure due to recrystallization phenomena, which in turn affects the austenite decomposition during water cooling. We apply method for calculating the austenite to bainite phase transformation onset for any cooling path for a steel of composition 0.09C, 0.2Si, 1.0Mn, 0.03Al, 1.1Cr, 0.18Mo, 0.026Ti, 0.0018B (wt. %) following deformation at different temperatures. The method is parameterized by constant cooling rate experiments to obtain the CCT diagram of this steel following deformation either above recrystallization limit temperature (*RLT*) or below the no-recrystallization temperature (T_{nr}). Using the CCT diagrams, we have performed analytical/numerical analysis of the transformation onset, which is based on the conversion of CCT to ideal TTT transformation diagram by the inversion of Scheil's additivity rule. After the conversion, the transformation onset can be calculated for any cooling path by applying Scheil's additivity rule. The analysis also provides information on the thermal activation parameters of the transformation onset. The discussion of the results is also provided.

Key words: Bainite, Deformation, Phase Transformation, Nucleation, CCT diagram, TTT diagram

1. INTRODUCTION

The final mechanical properties of a finished steel product depend on the thermomechanical procedure that has been applied in the processing of the steel (Kaijalainen et al., 2016; Kaijalainen et al., 2014; Kaijalainen et al., 2013). In the hot rolling mill practice this is achieved by controlling the rolling schedule and subsequent cooling path in the water cooling line. In order to have an efficient control of the manufacturing process, detailed real-time information is needed about various processing parameters that affect subsequent phase transformation during the cooling of the steel. During thermomechanical rolling, reductions, temperatures and time should be well controlled to achieve desired mechanical properties for strip. The model described in this article is intended to assist in defining cooling parameters of run out table in SSAB hot rolling mill at Raahe, Finland.

To model the bainite onset during phase transformation, the first step would be to develop CCT diagram for a given steel, thus simulating the thermomechanical processing to achieve desired austenite conditioning, followed by acquisitioning of data for phase transformation according to different linear cooling paths. This is followed by conversion of CCT to ideal TTT transformation diagram by the inversion of Scheil's additivity rule (Pham et al., 1995). In an earlier work (Pohjonen et al., 2016a), we have been able to successfully perform similar analytical/numerical analysis of the transformation onset of a carbon steel based on the principles of Scheil's additivity rule. After the conversion, the transformation onset can be calculated for any cooling path and can be fully coupled with, for example, a finite element simulation of temperature evolution inside the water cooled steel strip.

This analysis together with experimental observations allows us to discuss the factors affecting the

 ISSN 1641-8581

bainite transformation onset during cooling after deformation at different temperatures. The present analysis is part of an on-going research work which aims at full description of the transformation phenomena with the possibility of linking it to the heat conduction model to enable reading of real industrial data for user manipulation and process optimization (Pohjonen et al., 2016b). The analysis also provides a link between the experimental data and detailed microstructure models and can be used to determine possible range of values for the parameters in the comprehensive model.

2. EXPERIMENTAL PROCEDURE

To understand the onset of austenite to bainite transformation, a steel of the following composition was chosen (in wt. %): 0.09C, 0.2Si, 1.0Mn, 0.03Al, 1.1Cr, 0.18Mo, 0.026Ti, 0.0018B. The material was initially solution treated at 1250 °C for 2 hours, followed by water quenching. From the solution treated sample, cylindrical specimens of Φ 6 mm x 9 mm and Φ 4 mm x 6 mm were machined and used for the CCT dilatation tests at different linear cooling rates in the range 2-40 °C/s and 50-70 °C/s, respectively. To generate the dilatation data for constructing the CCT diagrams, continuous cooling experiments were performed in a Gleeble 3800 simulator according to two different programmed thermomechanical schedules: (a) deformation to 0.6 true strain above recrystallization limit temperature (RLT), and (b) deformation to 0.6 true strain below the no-recrystallization (T_{nr}) temperature.

Samples were heated at 10 °C/s to 1100 °C, held for 2 min, cooled to 850 °C, held 15 s, and then compressed with three hits each having a strain of ~0.2 at a strain rate of 1/s. The specimens were then held 5 s before cooling at various linear rates in the range 2–70 °C/s. For comparison, another set of specimens was reheated in a similar manner, held for 2 min prior to cooling at different linear cooling rates 2–70 °C/s. These two sets of simulation experiments were intended to simulate phase transformation characteristics both in strained (controlled rolling in the T_{nr} regime) and unstrained (finish rolling above RLT) conditions. Different phase transformation temperatures were identified from the temperature-dilatation data based on the deviation from the linear thermal contraction.

A general characterization of the transformation microstructures was performed with a laser scanning confocal microscope (VK-X200, Keyence Ltd.). Prior austenite grain sizes were measured as described in (Higginson & Sellars, 2003).

3. THEORY

If a TTT diagram of a given steel is known, an estimate for the onset of the transformation can be calculated by the application of the Scheil's additivity rule, Eq. (1), i.e. the transformation is assumed to start when the integral of fractional incubation times equals unity. In practice the integral can be evaluated by dividing the cooling path to small isothermal steps.

$$\int_0^{t_{onset}} \frac{1}{\tau(T(t))} = 1 \Rightarrow \sum_i \frac{t_i}{\tau(T)} = 1 \qquad (1)$$

here $t_i(T)$ is the time spent at temperature T and $\tau(T)$ is the required for the transformation to start during isothermal holding at temperature T. The value t_{onset} is the time required for the transformation to start during constant cooling, i.e. the time coordinate in the CCT diagram.

The constant cooling rate CCT diagram can be converted to the so-called ideal TTT diagram (Pham et al., 1995) by the inversion of the Scheil's additivity rule by applying Eq. (2).

$$\frac{1}{\tau(T_{cct})} = -\frac{d\dot{\theta}(T_{cct})}{dT_{cct}} \qquad (2)$$

where T_{cct} is the transformation temperature in the CCT diagram, $\dot{\theta}(T_{cct})$ is the cooling rate required for the transformation to start at T_{cct} and $\tau(T_{cct})$ is the ideal isothermal transformation start time at temperature T_{cct}. In practice, there is necessarily a slowest cooling rate in the experiments, causing the onset of the investigated transformation (austenite to bainite transformation in the current case).

Due to limited amount of experimental data, and the experimental inaccuracies, we used fitting function of the form of $\ln t_{85} = a \exp(bT)$ to interpolate the experimental CCT data. Here $t_{85} = 300 / \dot{\theta}(T_{cct})$. Applying Eq. (2) we obtain the ideal TTT function $\tau(T)$ described by Eq. (3)

$$\tau(T) = -\left[\frac{d}{dT}\frac{300}{t_{85}(T)}\right]^{-1} = ab\exp(a\exp(bT) - bT) \qquad (3)$$

Where a and b are fitting constants and t_{85} the cooling time between 800 and 500°C.

When using only interpolating function, Eq. (2) can only be used to calculate the ideal TTT diagram

for those temperatures, where the transformation starts during cooling with the experimental rates. In order to apply the Scheil's additivity rule also outside of the interpolated temperature range, extrapolation is necessary. For this we use functional form described by Zener-Hillert type equation, as reproduced in Eq. (4) (Borgenstam & Hillert, 2012):

$$\tau(T) = K(B_S - T)^{-m} \exp\left(\frac{Q}{R(T+273.15)}\right) \quad (4)$$

where K is a pre-factor, Q the activation energy of the rate limiting process, m a constant that depends on the rate determining process, Bs the bainite start temperature, and R the gas constant. Both m and Q in this study are determined by nonlinear least square fitting to the values obtained from Eq. (3). For this purpose we used MatLab lsqfit function (MatLab documentation). B_S is calculated by using Eq. (5) given by Steven and Haynes (1956):

$$B_S(°C) = 830 - 270w_C - 90w_{Mn} - 37w_{Ni} - 70w_{Cr} - 83w_{Mo} \quad (5)$$

The ideal TTT function $\tau(T)$ can then be used to calculate the transformation onset for any cooling path and it can be coupled with simulation of transient temperature field inside of a solid body by applying the Scheil's additivity rule, Eq. (1).

pancaking and effective grain boundary area (Higginson & Sellars, 2003). The S_v value determined for the pancaked samples deformed to 0.6 strain at 850 °C showed nearly double S_v value (253 μm^{-1}) compared to that of the recrystallized samples deformed at 1050 °C (117 S_v). The results of the CCT dilatation curves obtained for the two deformation conditions have been used in constructing the CCT diagrams and the same are reported elsewhere (Kaijalainen et al., 2017, in press). However, the relevant details of the CCT diagrams showing the bainite transformation behaviour for the two conditions have been reproduced in this paper in the form of an $\ln(t_{85})$ vs. temperature plot, for favour of the required analysis and modelling, as described below.

A comparison of the experimental CCT data corresponding to the bainitic transformation and the fitted exponential functions is shown in figure 2. The fitting constants a and b mentioned above were derived from the $\ln t_{85}$ vs. temperature plots, as shown in the figure. The corresponding fitting parameters for the recrystallized specimens (deformed at 1050 °C) are: $a_1 = 3.9770 \times 10^{-3}$ and $b_1 = 1.2149 \times 10^{-2}$ and those corresponding to the strained specimens (deformed in the T_{nr} regime at 850 °C) are: $a_2 = 1.0771 \times 10^{-2}$ and $b_2 = 9.8212 \times 10^{-3}$ (here, suffixes 1 and 2 essentially distinguish between the parameters pertaining to recrystallized and strained specimens, respectively). Whereas the fitting constant b is quite close for the two cases, the constant a has been found to be nearly 2.5 times higher for the strained specimens. The regression fitting shown in figure 2 has been found to be quite good; the coefficient of determination $r^2 \approx 0.9$ for both the cases.

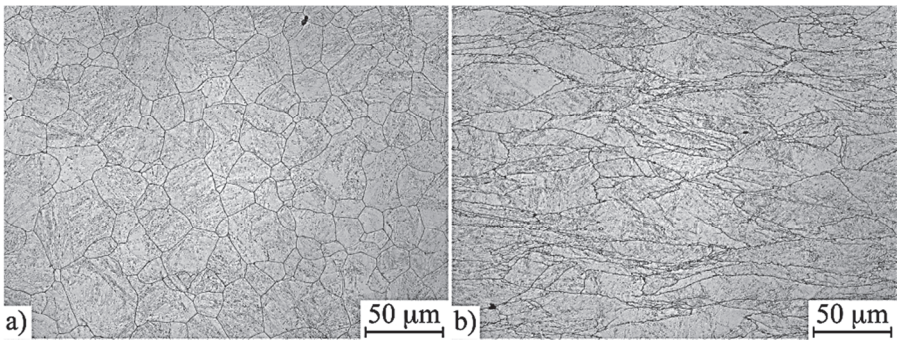

Fig. 1. *Prior austenite grain structures following deformation to 0.6 true strain: (a) above RLT (1050 °C) and (b) below the T_{nr} temperature (850 °C).*

4. RESULTS AND DISCUSSION

The microstructures recorded on a laser confocal microscope for the samples deformed in the recrystallization regime (above RLT) and below T_{nr} temperature are shown in figure 1. Whereas the samples deformed above RLT show fully recrystallized, equiaxed grains of an average grain size ≈17 µm, the samples deformed below T_{nr} temperature showed distinctly pancaked grains with comparable grain size (≈12 µm), though some grains were relatively coarse. Even more interesting is the surface area per unit volume (S_v), which is an index of the extent of

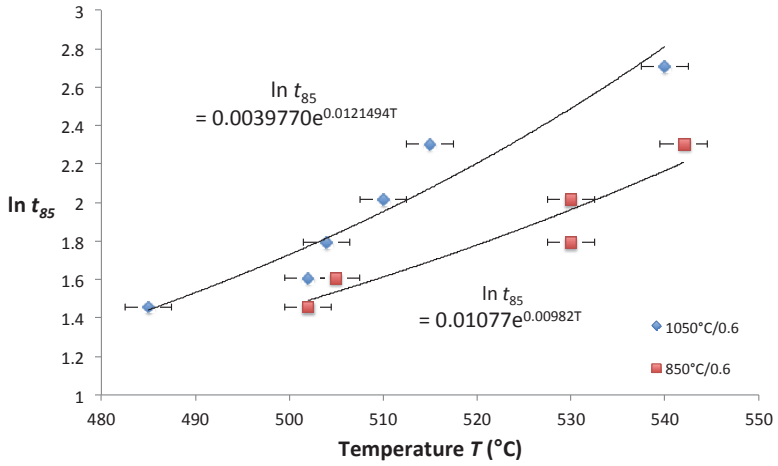

Fig. 2. *Plot of ln t_{85} versus T. Due to limited amount of experimental data and the experimental inaccuracy, a fitting function ln t_{85} = a exp(bT) was used for interpolation*

Table 1. *Comparison of the values obtained in the current study to other similar values described in the literature. (a) Pham et al., 1995; b) Li et al., 1998; c) Kirkaldy & Venugopalan, 1983; d) Kang et al., 2009)*

Steel	m	Q (kJ/mol)	Transformation product	Reference
0.82C-0.88Mn-0.28Si	4.15	125	Pearlite	a)
Median for several steels	2	115	Bainite	b)
Median for several steels	3	115	Ferrite	b)
Median for several steels	3	115	Pearlite	b)
Optimal fit to many steels	2	115	Bainite	c)
Optimal fit to many steels	3	98	Ferrite	c)
1.13 wt. % C steel	-	127	Upper bainite (8 % transformed)	d)
1.13 wt. % C steel	-	52	Lower bainite (8 % transformed)	d)
0.77 wt. % C steel	-	77	Upper bainite (8 % transformed)	d)
0.77 wt. % C steel	-	35	Lower bainite 8 % transformed)	d)
See text	3.0	75.5	Bainite onset (Recrystallized matrix)	Current work
See text	1.5	37.9	Bainite onset (Strained matrix)	Current work

The calculated TTT plots, obtained either with Eq. (3) or Eq. (4) (plots indistinguishable) are shown in figure 3. We obtained the values Q=75.4 kJ/mol, m≈3.0 and K=13.3 for the steel deformed at 1050 °C and corresponding values for the steel deformed at 850 °C were: Q=37.9 kJ/mol, m=1.5 and K=4.5, thus revealing a large influence of straining in the matrix on the bainite onset parameters. For comparison, corresponding values for different transformation products including bainite taken from other sources in literature are reproduced in table 1.

The comparison clearly shows that the values for activation energy Q and exponent m obtained in this study are fairly reasonable. Of interest is the variation in the value of Q, which points to the possibility of formation of different types of bainite (upper or lower) for the two prior conditions of straining resulting in strained and recrystallized states. This, however, is related to the transformation temperature that can vary as a function of cooling rate and the activation energies reported in this study are of overall nature as also reported elsewhere (a) Pham et al., 1995; b) Li et al., 1998; c) Kirkaldy & Venugopalan, 1983; d) Kang et al., 2009) and is beyond the scope of this work.

Both the activation energy of bainite transformation Q and exponent m are nearly half for the strained specimens in comparison to those of the recrystallized samples. The prefactor K has been found to be nearly three times higher for the recrystallized condition (13.3) compared to that in strained condition (4.5), even though the average grain size for recrystallized structure is relatively fine. However, taking into account the large number of dislocation substructures, low angle boundaries and slip bands, in addition to the high S_v (253 μm^{-1}) that has been obtained during straining at 850 °C, the effective grain size would be much finer keeping in view the possibility of heterogeneous nucleation of bainite on slip bands and other deformation heterogeneities (Bhadeshia, 2001). This could be one reason that the activation energy of transformation for strained samples showing pancaked grains is relatively lower. The exponential factor m depends on the transformation process. For diffusional transformation, the value has been linked to effective diffusion mechanism, for example, m=2 for volume diffusion and m=3 for boundary diffusion in the case of pearlite transformation (Li et al., 1998; Kirkaldy & Venugopalan, 1983). Table 1 compiles m values for different steels in the range 2-4 irrespective of the type of transformation, which suggests that there is a likelihood of volume ($m \leq 2$)

and boundary ($m \geq 3$) diffusion in different cases. Though bainite transformation is considered to be of displacive nature, but the concurrent growth of bainitic laths and diffusion of carbon, or for that matter, limited diffusion of substitutional elements can also take place because of the high transformation tempertatures compared to that of martensite transformation (Liang & DeArdo, 2014). Thus the m values obtained in our case tentatively signify the occurrence of boundary diffusion ($m = 3$) and volume diffusion ($m = 1.5$) as primary mechanisms operating in the case of recrystallized and strained samples, respectively.

The microstructures corresponding to the cooling rates in the range 20-70 °C/s are reported elsewhere (Kaijalainen et al., 2017, in press), which show lower bainite in both cases, even though the bainite onset conditions are somewhat different for the two conditions (recrystallized and strained). Apparently it seems that the lowering of activation energy in the case of strained samples is tentatively due to extensive pancaking and increase in effective grain boundary area.

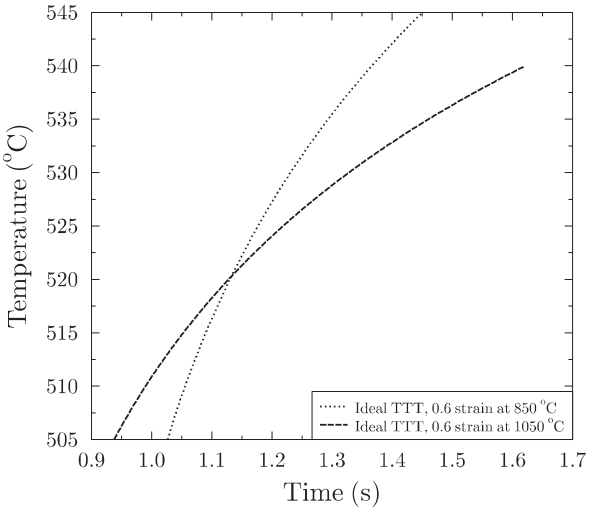

Fig. 3. *Comparison of the ideal TTT diagrams calculated using Eq. (2) or (4) (the plots from either of the two equations could not be distinguished in a figure) for the investigated steel subjected to 0.6 true strain at either 850 °C or 1050 °C.*

Using the obtained values for Q, m and K together with Eq. (1), (4) and (5), the transformation start can now be calculated for any cooling path. The calculation can further be coupled to heat conduction simulations. Also, the analysis presented in this article provides information for more detailed microstructure simulations, because the possible range for the parameters in such simulations must be compatible with the experimental data and analysis presented here.

5. CONCLUDING REMARKS

We have analyzed experimental continuous cooling data of bainite onset in order to transform it to the ideal TTT diagram. Zener-Hillert type equation has been fitted to the obtained ideal TTT diagram. Since the fitted parameters obtained by applying the equation are comparable to the values reported in the literature, we presume that the parameters adequately describe the transformation onset and can be applied further to calculate the bainite transformation onset for any cooling path. The values and the interpretation of the parameters can be used in construction of more detailed microstructure models describing the onset of the transformation.

The effective activation energy of the rate limiting process for the strained samples was nearly half of the corresponding value obtained for the recrystallized sample. Also, the prefactor K of the strained sample was found to be about one third of the value obtained for the recrystallized samples, suggesting that there are more sites available for bainite nucleation in the strained samples. The analysis of the exponential factor m based on literature information tentatively suggests that volume diffusion type mechanism may be the primary rate limiting process in the case of the strained samples, in contrast to the possibility of boundary diffusion as the rate limiting process in the case of recrystallized samples.

REFERENCES

Bhadeshia, H. K. D. H., 2001, *Bainite in Steels*, The University Press, 215.

Borgenstam, A., Hillert, M., 2012, Kinetics of Bainite Transformation in Steels, *Phase Transformations in Steels*, eds, Pereloma, E., Edmonds, D., V., (editors), Woodhead Publishing Limited.

Higginson, R. L., Sellars, C. M., 2003, *Worked Examples in Quantitative Metallography*, Maney Publishing, London.

Kaijalainen, A., Liimatainen, M., Kesti, V., Heikkala, J., Liimatainen, T., Porter, D. A., 2016, Influence of Composition and Hot Rolling on the Subsurface Microstructure and Bendability of Ultrahigh-Strength Strip, *Metallurgical and Materials Transactions, A*47A, 4175-4188.

Kaijalainen, A., Suikkanen, P., Karjalainen, P., Jonas, J. J., 2014, Effect of Austenite Pancaking on the Microstructure, Texture, and Bendability of an Ultrahigh-Strength Strip, *Metallurgical and Materials Transactions A*, 45, 1273-1283, DOI 10.1007/s11661-013-2062-7.

Kaijalainen, A., Suikkanen, P., Limnell, T. J., Karjalainen, L. P., Kömi, J. I., Porter, D. A., 2013, Effect of austenite grain structure on the strength and toughness of direct-quenched martensite, *Journal of Alloys and Compounds*, 577, S642-S648.

Kaijalainen, A., Vähäkuopus, N., Somani, M., Mehtonen, S., Porter, D., Kömi, J., 2017, The Effects of Finish Rolling Temperature and Niobium Microalloying on the Microstructure and Properties of a Direct Quenched High-Strength Steel, *Archives of Metallurgy and Materials*, 62, 1 (in press).

Kang, M., Zhang, M-X., Liu, F., Zhu, M., 2009, Kinetics and Morpology of Isothermal Transformations at Intermediate Temperature in 15CrMnMoV Steel, *Materials Transactions*, 50, 1, 123-129.

Kirkaldy, J. S., Venugopalan, D., 1983, Prediction of Microstructure and Hardenability in Low Alloy Steels, in *Phase Transformations in Ferrous alloys*, eds., Marder, D. A. R, Goldstein, J. I., AIME, New York, NY, 125-148.

Li, V. M., Niebuhr, D. V., Meekisho L. L., Atteridge, D. G., 1998, A Computational Model for the Prediction of Steel Hardenability, *Metallurgical and Materials Transactions B*, 29B, 661-672.

Liang, X., DeArdo, A. J., 2014, A Study of the Influence of Thermomechanical Controlled Processing on the Microstructure of Bainite in High Strength Plate Steel, *Metallurgical and Materials Transactions A*, 45, 11, 5173-5184.

MatLab documentation, available online at: http://se.mathworks.com/help/matlab/ accessed: 2.01.2017.

Pham, T.T., Hawbolt, E.B., Brimacombe, J.K., 1995, Predicting the Onset of Transformation under Noncontinuous Cooling Conditions: Part II. Application to the Austenite Pearlite Transformation, *Metallurgical and Materials Transactions*, 1995*A*, 26A, 1993-2000.

Pohjonen, A., Somani, M., Pyykkönen, J., Paananen, J.,Porter, D., 2016a, The Onset of the Austenite to Bainite Phase Transformation for Different Cooling Paths and Steel Compositions, *Key Engineering Materials*, 716, 368-375.

Pohjonen, A., Kyllönen, V., Paananen, J., 2016b, Analytical Approximations and Simulation Tools for Water Cooling of Hot Rolled Steel Strip, *Proceedings of the 9th EUROSIM Congress on Modelling and Simulation*, 731-736 DOI 10.1109/EUROSIM.2016.42.

Steven W., Haynes A.G., 1956, The temperature of formation of martensite and bainite in low-alloy steels, *J. Iron Steel Inst.,* 183, 349-359.

ANALIZA POCZĄTKU PRZEMIANY BAINITYCZNEJ PODCZAS CHŁODZENIA PO ODKSZTAŁCENIU W RÓŻNYCH TEMPERATURACH

Streszczenie

Temperatura końca walcowania ma wpływ na przebieg rekrystalizacji i na mikrostrukturę austenitu, która w konsekwencji oddziałuje na kinetykę rozpadu austenitu w czasie chłodzenia wodą. W niniejszej pracy przedstawiono metodę obliczania temperatury przemiany austenit-bainit po odkształceniach w różnych temperaturach. Analizowano stal zawierającą 0.09C, 0.2Si, 1.0Mn, 0.03Al, 1.1Cr, 0.18Mo, 0.026Ti, 0.0018B (% wagowe). Współczynniki w opracowanym modelu wyznaczono na podstawie wykresów CCT otrzymanych z doświadczeń przeprowadzanych przy stałej prędkości chłodzenia. Wykresy sporządzono dla stali odkształconej wcześniej w temperaturze powyżej temperatury rekrystalizacji (ang. recrystallization limit temperature - RLT) oraz poniżej temperatury zatrzymania rekrystalizacji (Tnr). Wykorzystując otrzymane wykresy CCT przeprowadzono analityczno/numeryczną analizę początku przemiany, która stanowiła podstawę do przekształcenia wykresu CCT w idealny wykres TTT. Wykorzystano tutaj odwrotną regułę addytywności Scheila. Po tym przekształceniu, stosując prostą regułę addytywności, początek przemiany może być obliczony dla dowolnego przebiegu cyklu chłodzenia. Przeprowadzona analiza dostarczyła danych o aktywowanych cieplnie parametrach modelu przemiany. Pracę podsumowuje dyskusja wyników.

Received: November 15, 2016
Received in a revised form: November 30, 2016
Accepted: December 16, 2016